



PERGAMON

Solid State Communications 110 (1999) 525–530

solid  
state  
communications

## Phase diagram for $\text{Ca}_{1-x}\text{Y}_x\text{MnO}_3$ type crystals

H. Aliaga, R. Allub\*, B. Alascio

*Centro Atómico Bariloche, (8400) S. C. de Bariloche, Argentina*

Received 22 April 1998; accepted 2 December 1998 by C.E.T. Gonçalves da Silva

### Abstract

We present a simple model to study the electron doped manganese perovskites. The model considers the competition between double exchange mechanism for itinerant electrons and antiferromagnetic superexchange interaction for localized electrons. It represents each  $\text{Mn}^{4+}$  ion by a spin  $1/2$ , on which an electron can be added to produce  $\text{Mn}^{3+}$ ; we include a hopping energy  $t$ , a strong intratomic ferromagnetic interaction exchange  $J$  (in the limit  $J/t \rightarrow \infty$ ), and an interatomic antiferromagnetic interaction  $K$  between the local spins. Using the Renormalized Perturbation Expansion and a Mean Field Approximation on the hopping terms and on the superexchange interaction, we calculate the free energy. From it, the stability of the antiferromagnetic, canted, ferromagnetic, and novel spin glass phases can be determined as functions of the parameters characterizing the system. The model results can be expressed in terms of  $t$  and  $K$  for each value of the doping  $x$  in phase diagrams. The magnetization  $m$  and canting angle  $\theta$  can also be calculated as functions of temperature for fixed values of doping and model parameters. © 1999 Elsevier Science Ltd. All rights reserved.

*Keywords:* A. Magnetically ordered materials; D. Electronic transport

### 1. Introduction

The discovery of “colossal” magnetoresistance (CMR) in  $\text{La}_{1-x}\text{Sr}_x\text{MnO}_3$  type compounds [1] together with its many unusual properties have attracted considerable attention. The phase diagram, as a function of concentration  $x$ , temperature, magnetic field, or magnitude of the superexchange interaction is not quite clear yet for the different compounds.

Before the discovery of CMR, Jonker and Van Santen [2,3] established a temperature-doping phase diagram separating metallic ferromagnetic from insulating antiferromagnetic phases. Zener [4] proposed a ‘Double Exchange’ (DE) mechanism to understand the properties of these compounds and the connection

between their magnetic and transport properties. This DE mechanism was used by Anderson and Hasegawa [5] to calculate the ferromagnetic interaction between two magnetic ions, and by de Gennes [6] to propose canting states for the weakly doped compounds. Kubo and Ohata [7] used a spin wave approach to study the temperature dependence of the resistivity at temperatures well below the critical temperature and a mean field approximation at  $T$  near  $T_c$ . Mazzaferro, Balseiro and Alascio [8] used a mixed valence approach similar to that devised for TmSe combining DE with the effect of doping to propose the possibility of a metal insulator transition in these compounds. Furuwaka [9] has shown that DE is essential to the transport theory of these phenomena, while Millis et al. [10] have argued that DE alone is not sufficient to describe the properties of some of the alloys under consideration and have proposed that lattice polaronic effects play an important role. In a previous paper we have shown

\* Member of the Carrera del Investigador Científico del Consejo Nacional de Investigaciones Científicas y técnicas (CONICET).

*E-mail address:* allub@cab.cnea.edu.ar (R. Allub)

that a semi-phenomenological model, which includes the effect of the disorder introduced by doping, can explain the transport properties of  $\text{La}_{1-x}\text{Sr}_x\text{MnO}_3$  [11,12].

In [11,12] we treat the Hamiltonian proposed for these systems using an alloy analogy approximation to the exchange terms and including the effects of disorder by introducing a continuous distribution of the diagonal site energies. Since the focus of the paper was on transport properties of the ferromagnetic materials, we emphasize the disorder aspects of the problem and ignore interactions that would give rise to phases other than ferromagnetic.

Here we propose to extend the previous studies to the region of concentration of dopant where the antiferromagnetic interactions, always present, compete with double exchange. We will focus on the Ca rich end of  $(\text{RE})_x\text{Ca}_{1-x}\text{MnO}_3$  compounds (where RE stands for rare earths) because the antiferromagnetic order is simpler in these alloys. To simplify the problem, we start in this paper by ignoring disorder effects to study the thermodynamical stability of different phases.

## 2. Model

The system in consideration contains two kinds of magnetic ions:

$\text{Mn}^{4+}$  with three localized  $t_{2g}$  electrons giving rise to a spin 3/2. We will refer to these electrons as the ‘‘localized spin’’ electrons.

$\text{Mn}^{3+}$ , which besides the localized spin, contains an itinerant electron in the  $\varepsilon_g$  orbitals. Due to the strong intra atomic exchange coupling  $J$ , this  $\varepsilon_g$  electron couples ferromagnetically ( $J > 0$ ) to the localized spin to produce a spin two at these sites. For  $U = K = 0$ , and  $J < 0$  the model would represent the Kondo lattice. For this reason the problem is sometimes erroneously referred to as the ‘‘Ferromagnetic Kondo Lattice’’. One should be aware however that none of the subtle physics of the Kondo problem is present if the localized-itinerant spin interaction is ferromagnetic.

The itinerant electron can jump, conserving spin from site to site, with hopping energy  $t$ . These processes give rise to the double exchange mechanism, making the system transport properties

metallic-like and trying to order the spins ferromagnetically. It is easy to estimate the energy gain in the ferromagnetic state due to this process as being of the order of the hopping energy  $t$  times the doping  $x$ .

Superexchange between localized spins gives rise to an antiferromagnetic coupling  $K$  that competes with double exchange and can lead to different phases. We investigate here the stability of canted, ferro and antiferromagnetic phases. To this end, we divide the Mn lattice in two interpenetrating sublattices appropriate to describe type G antiferromagnetism [13] which is known to be stable at the Ca-rich end of the composition. We indicate by *I* or *II* the sites belonging to each sublattice, and define a quantization axis for each sublattice.

According to the above considerations we write the following model Hamiltonian:

$$H = \sum_{i,\sigma} \varepsilon_i n_{i,\sigma} + U \sum_{i,\sigma} n_{i,\sigma} n_{i,-\sigma} - J \sum_i \mathbf{S}_i \cdot \boldsymbol{\sigma}_i + K \sum_{\langle i,j \rangle} \mathbf{S}_i \cdot \mathbf{S}_j + \sum_{\langle i,j \rangle, \sigma} t_{ij} (c_{i\sigma}^+ c_{j\sigma} + h.c.),$$

where  $n_{i,\sigma} = c_{i\sigma}^+ c_{i\sigma}$ , and  $c_{i\sigma}^+$ ,  $c_{i\sigma}$  creates and destroys an itinerant electron with spin  $\sigma$  at site  $i$ , respectively.  $\mathbf{S}_i$  and  $\boldsymbol{\sigma}_i$  are the localized and itinerant spin operators at site  $i$ , respectively.  $\varepsilon_i$  are the site diagonal energies,  $U$  is the intra-atomic electronic repulsion, and  $t_{ij}$  is the hopping parameter between nearest neighbors sites  $i,j$ .

To simplify the mathematical treatment, we take only the  $z$  component of the  $\mathbf{S}_i \cdot \boldsymbol{\sigma}_i$  interaction and we replace  $\mathbf{S}_i \cdot \mathbf{S}_j$  by  $S_{z,i} \langle S_{z,j} \rangle + S_{z,j} \langle S_{z,i} \rangle - \langle S_{z,j} \rangle \langle S_{z,i} \rangle$ .

After doing this, the Hamiltonian  $H$  can be separated into a local  $H_0$  given by

$$H_0 = \sum_{i,\sigma} \varepsilon_i n_{i,\sigma} + U \sum_{i,\sigma} n_{i,\sigma} n_{i,-\sigma} + J \sum_i S_{z,i} \sigma_{z,i} + K \sum_i S_{z,i} \cdot \sum_j \langle S_{z,j} \rangle$$

and a non-local

$$H_1 = \sum_{\langle i,j \rangle, \sigma} t_{ij} (c_{i\sigma}^+ c_{j\sigma} + h.c.)$$

To reduce the mathematical complexity of the problem to a minimum we make the following additional simplifications: (a) We represent the lattice as

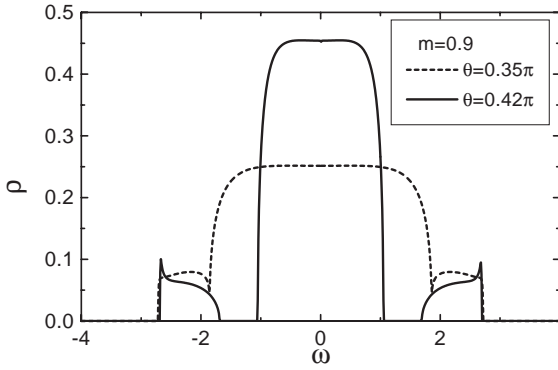


Fig. 1. Total density of states vs energies ( $\omega$ ) for  $kt = 5$ ,  $m = 0.9$ , and two different values of the canting angle in the region  $\pi/4 \leq \theta \leq \pi/2$ . The “side” bands are related with a process of hopping electron between a localized spin oriented parallel to its direction of quantization (+) and a first neighbor localized spin oriented antiparallel to its corresponding quantization direction (-).

two interpenetrating sublattices ( $I$  and  $II$ ) in which we define quantization axes forming an angle  $2\theta$  between them (b) We represent the localized spin to be  $\frac{1}{2}$ , so that they can be parallel or antiparallel to the local quantization direction on each sublattice. (c) Coulomb repulsion  $U$  and exchange  $J$  are much larger than  $t_{ij}$  and taken to be infinite here. Finite  $U$  and  $J$  lead to effective antiferromagnetic coupling between  $Mn^{3+}$  ions and compete in the La-rich side of the alloys with the ferromagnetic coupling due to double exchange. The large  $U$  limit precludes occupation of the  $\epsilon_g$  orbitals at each site by more than one itinerant electron. (d) In accordance with one of the fundamental points of DE mechanism, [5] we take the semiclassical approximation for the hopping energy:  $t_{ij} = t \cdot \cos(\theta)$ , where  $\theta$  is half the angle between localized spin directions in  $I$  and  $II$  sublattices. (e) The diagonal energies  $\epsilon_i$  are all equal and define the zero of one-particle energies. Chemical disorder, which is present in real samples and fundamental to the transport properties, is ignored in this first approach. The effect of disorder in the thermodynamic properties is not crucial to the ordered phases and can be estimated at large disorder by replacing the hopping energy  $t$  by  $(t^2/\Gamma)$  where  $\Gamma$  measures the width of the energy distribution [14]. (f) We ignore lattice dynamics that could give rise to polaronic effects. These phenomena have been discussed by [10] and

references therein. When necessary, they may be included a posteriori.

### 3. Results and discussion

In order to obtain the density of states for itinerant electrons, we have to calculate local Green’s functions. To obtain the local Green’s functions, we resort to the same procedure as in [11,12] and [8] and work on a interpenetrating Bethe lattice. The itinerant electrons spin up Green’s functions corresponding to  $H_0$  at a local spin up site is given by

$$G_{i\uparrow\alpha}^{0l} = \langle\langle c_{i\uparrow}; c_{i\uparrow}^\dagger \rangle\rangle = \frac{[\omega - E_\alpha - U(1 - \bar{n}_{i\uparrow})]}{(\omega - E_\alpha)(\omega - E_\alpha - U)},$$

where  $\bar{n}_{i\uparrow} = \langle c_{i\uparrow}^\dagger c_{i\uparrow} \rangle$ ,  $\alpha = + (-)$  for up (down) localized spin,  $l$  is the sublattice index ( $I, II$ ), and  $E_\alpha = \epsilon - \alpha J$ , which for large  $J$  and  $U$  reduces at the lowest energy pole to  $G_{i\uparrow\alpha}^{0l} = \delta_{\alpha+}/(\omega - \epsilon + J)$ , which from here on we take at zero ( $\epsilon = J$ ) and where  $\delta_{++} = 1$  and  $\delta_{-+} = 0$ . We ignore the upper pole as it becomes irrelevant to the problem in consideration (electron concentration  $x < 1$ ).

The Renormalized Perturbation Expansion (RPE) [15] as in [11,12] connects the propagator at site  $i$  to propagators at the nearest neighbor sites  $i + \delta$  which exclude visiting site  $i$  again and which we will denote by small  $g$ ’s. These new propagators are in turn connected to propagators of the same type at sites  $i + \delta + \delta'$  etc., so that Green’s function at each site depends, through this chain, on local spin configuration because of the factors  $\delta_{\alpha+}$ .

The defined chain of equations reads for example:

$$G_{i\uparrow+}^I = \frac{1}{\omega - \Delta_{i\uparrow+}^{I+}}, \tag{1}$$

where the self energy  $\Delta_{i\uparrow+}^{I+}$  is

$$\Delta_{i\uparrow+}^{I+} = \sum_{\delta} t_{i,i+\delta}^2 g_{i+\delta\uparrow}^{II}, \tag{2}$$

in terms of the modified Green’s functions  $g_{i+\delta\uparrow}^{II}$  at the other sublattice, and

$$g_{i+\delta\uparrow}^{II} = \frac{\delta_{\alpha+}}{\omega - \Lambda_{i+\delta\uparrow}^{II\alpha}}, \tag{3}$$

where  $\Lambda$  are the self energies of the new Green’s

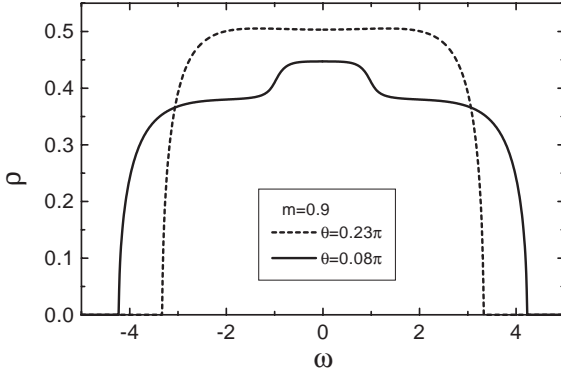


Fig. 2. Total density of states as a function of  $\omega$  for  $k/t = 5$ ,  $m = 0.9$ , and two different values of the canting angle in the region  $0 \leq \theta \leq \pi/4$ .

functions  $g$ , which are given in turn by:

$$\Lambda_{i+\delta\uparrow}^{II\alpha} = \sum_{\delta'} t_{i+\delta, i+\delta+\delta'}^2 g_{i+\delta+\delta'\uparrow}^I, \quad (4)$$

and,

$$g_{i+\delta+\delta'\uparrow}^I = \frac{\delta_{\alpha+}}{\omega - \Lambda_{i+\delta+\delta'\uparrow}^{I\alpha}}, \quad (5)$$

$$\Lambda_{i+\delta+\delta'\uparrow}^{I\alpha} = \sum_{\delta''} t_{i+\delta+\delta', i+\delta+\delta'+\delta''}^2 g_{i+\delta+\delta'+\delta''\uparrow}^{II}, \quad (6)$$

etc.

As mentioned above, this procedure leads to different Green's functions for different sites, according to the local spin configuration around the site. We are interested in the configurational average of  $G_{i\sigma\alpha}^I$  over all possible spin configurations:  $G_{\alpha}^I = \langle G_{i\sigma\alpha}^I \rangle$  which is independent of  $i$  and different from zero only for  $\sigma = \alpha$ . This configurational average over local spin directions is assumed to be the same at every site of the same sublattice, to restore translational invariance in the spirit of the mean-field theories as ATA, CPA, etc. Thus in Eq. (2) for example, we assume that at in all sites the sum over neighbors can be replaced by an average number of neighbors with subindex  $+$  equal to  $(k+1)$  times the probability of local spin up at lattice  $II$ ,  $\nu_+$ , leading to the Eq. (8) below. We use the same procedure to the previous set of equations. To this purpose, we define the magnetization  $m$  to characterize the

background of localized spins at the lattice sites and we introduce the probability  $\nu_{\alpha} = (1 + \alpha m)/2$  that a site has parallel ( $\alpha = +$ ) or antiparallel ( $\alpha = -$ ) localized spin to the quantization axes in each sublattice and we write:

$$G_{\alpha}^I = \frac{\nu_{\alpha}}{\omega - \Delta^{I\alpha}}, \quad (7)$$

$$\Delta^{I\alpha} = (k+1)t^2(\cos^2(\theta)g_{\alpha}^{II} + \sin^2(\theta)g_{-\alpha}^{II}), \quad (8)$$

$$G_{\alpha}^{II} = \frac{\nu_{\alpha}}{\omega - \Delta^{II\alpha}}, \quad (9)$$

$$\Delta^{II\alpha} = (k+1)t^2(\cos^2(\theta)g_{\alpha}^I + \sin^2(\theta)g_{-\alpha}^I), \quad (10)$$

$$g_{\alpha}^{II} = \frac{\nu_{\alpha}}{\omega - \Lambda^{II\alpha}}, \quad (11)$$

$$\Lambda^{II\alpha} = kt^2(\cos^2(\theta)g_{\alpha}^I + \sin^2(\theta)g_{-\alpha}^I), \quad (12)$$

$$g_{\alpha}^I = \frac{\nu_{\alpha}}{\omega - \Lambda^{I\alpha}}, \quad (13)$$

$$\Lambda^{I\alpha} = kt^2(\cos^2(\theta)g_{\alpha}^{II} + \sin^2(\theta)g_{-\alpha}^{II}), \quad (14)$$

Eliminating the self-energies and using the symmetry between lattices  $I$  and  $II$ , the former equations can be reduced to two interconnected equations:

$$g_{\pm} = \frac{\nu_{\pm}}{\omega - kt^2(\cos^2(\theta)g_{\pm} + \sin^2(\theta)g_{\mp})}, \quad (15)$$

from which we finally obtain:

$$G_{\alpha} = \frac{\nu_{\alpha}}{\omega - (k+1)t^2(\cos^2(\theta)g_{\alpha} + \sin^2(\theta)g_{-\alpha})}, \quad (16)$$

where  $(k+1)$  is the number of nearest neighbors (six for the simple cubic Mn lattice).

Solving Eqs. (15) and (16) allows us to obtain the densities of states per site  $\rho(m, \theta, \omega) = \rho_+(m, \theta, \omega) + \rho_-(m, \theta, \omega)$ , with  $\rho_{\pm}(m, \theta, \omega) = \text{Im}(G_{\pm})/\pi$ .

For  $m = 0$ , we obtain the paramagnetic case:  $G_- = G_+$  given by

$$G_+ = \frac{0.5}{\omega - \frac{(k+1)}{2k}(\omega + \sqrt{\omega^2 - 2kt^2})}.$$

As expected, we see that  $G_{\pm}$  is independent of the canting angle and the band-width reduces to  $(2\sqrt{2}kt^2)$ .

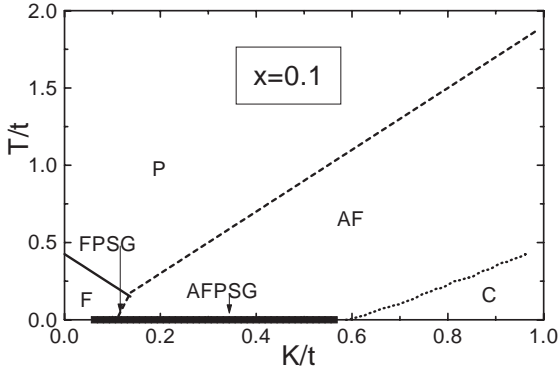


Fig. 3. Phase diagram  $T/t$  vs  $K/t$ , with a  $x = 0.1$  electrons/site. Different phases appears: paramagnetic (P), ferro (F), antiferro (AF), canted (C) and pseudo spin glass (FPSG and AFPSG). Transitions into the P phase are second order. All others transitions are first order.

For  $m = 1$ , the extreme order case occur:  $G_- = 0$  and  $G_+$  reduces to

$$G_+ = \frac{1}{\omega - \frac{(k+1)}{2k}(\omega + \sqrt{\omega^2 - 4kt^2 \cos^2(\theta)})}$$

this Eq. shows that the maximum band-width occur for the ferromagnetic case ( $\theta = 0$ ), this is in agreement with the result of Ref. [9]. For  $\theta = \pi/2$ , we

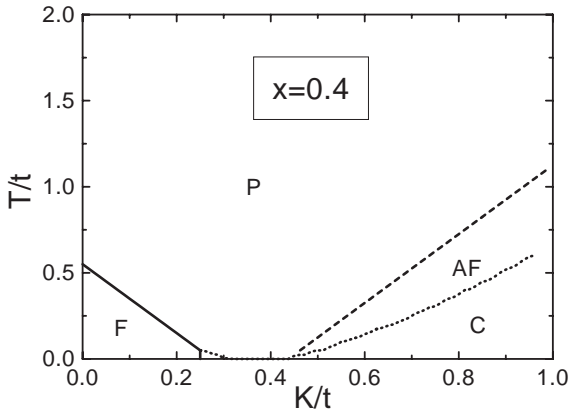


Fig. 4. Phase diagram  $T/t$  vs  $K/t$ , with a  $x = 0.4$  electrons/site. For this concentration, the kinetic energy is the lowest and then the PSG phases dissappear. We can see paramagnetic (P), ferro (F), antiferro (AF), and canted (C) phases only. Transitions into the P phase are second order. All others transitions are first order. Note the interphase between F and C phases.

obtain the antiferromagnetic case and the density of states reduces to the delta function.

For  $0 < m < 1$ ,  $\rho$  shows two different pictures according to the canting angle  $\theta$ : (a) for  $\pi/2 \geq \theta \geq \pi/4$ , we have a density of states with a central one and two lateral bands as shown in Fig. 1. (b) for  $\pi/4 \geq \theta \geq 0$ , we have a single band structure similar to the ferromagnetic case obtained in [11,12] and the bandwidth decreases with  $\theta$ . We show this band structure in Fig. 2.

The density of states allows us to write  $x = \int_{-\infty}^{\epsilon_F} \rho(m, \theta, \omega) d\omega$ .

For a fixed value of doping  $x$ , this equation determines the Fermi energy  $\epsilon_F$ . Henceforth, we take  $k = 5$  and the hopping energy  $t = 1$ .

The kinetic energy is given by  $E_{kin}(m, \theta, x) = \int_{-\infty}^{\epsilon_F} \rho(m, \theta, \omega) \omega d\omega$ , where we use the average sublattice magnetization and the canting angle as order parameters. The thermodynamical values of  $m$  and  $\theta$  correspond to the minimum of the free energy given by  $F = E_{kin}(m, \theta, x) + E_K(m, \theta, K) - T \cdot S(m)$ , where  $E_K(m, \theta, K)$  is the antiferromagnetic superexchange energy related to the localized spins and given in mean field approximation by  $E_K(m, \theta, K) = Km^2 \cos(2\theta)$  and  $S(m)$  is the entropy term, and we take the simplest possible form compatible with our earlier approximations:  $S(m) = \ln(2) - \nu_+ \ln(2\nu_+) - \nu_- \ln(2\nu_-)$ . More accurate forms of the entropy valid in the mixed valence regime can be used. See, for example, Ref. [16,17].

At zero temperature, the phase diagram is dominated by the competition between the DE mechanism and the superexchange energy. For  $K \ll t$ , the kinetic energy is the most important term in the ground state energy and the minimum corresponds to  $m = 1$  and  $\theta = 0$  which define the ferromagnetic phase (F). For  $K \gg t$ , the relevant term emerges from the superexchange interactions and the minimum corresponds to  $m = 1$  and  $\theta = \pi/2$  which define the antiferromagnetic phase (AF). When  $K$  and  $t$  have the same order, competition between both energies takes place and a phase which we call pseudo spin glass (PSG), defined by  $m < 1$ , appears. We obtain two different PSG phases according to the value of  $K/t$ . So that, starting from the F phase and increasing  $K$ , we obtain first a ferromagnetic pseudo spin glass (FPSG) characterized by  $\theta = 0$ , and then a second transition into an antiferromagnetic pseudo spin

glass (AFPSG) with  $\theta = \pi/2$ . Finally, starting from the AFPSG and increasing  $K$ , we observe the canted phase (C), where the minimum corresponds to  $m = 1$  and  $\theta < \pi/2$  (as  $K$  increases,  $\theta \rightarrow \pi/2$ ). Figs. 3 and 4 show this behaviour for two values of the concentration. PSG phases reduce with  $x$  and disappear for  $x = 0.4$  as shown in Fig. 4.

The presence of the PSG phases, both in the ferro- and antiferromagnetic regimes suggests that the competition between DE and SE interactions gives rise to frustration rather than to the canted state. This differs from the results obtained by Arovas and Guinea [18] who used a Schwinger boson formalism to describe hole doped  $\text{LaMnO}_3$ . However, the phase diagram obtained here, is very similar to that obtained by Golosov et al. [19]. Both this treatment and ours allow for local distortions of the spin arrangement to lower the kinetic energy of itinerant electrons; we think that the PSG state is a state where local distortions appear in the ferro- or antiferromagnetic phases.

At finite temperature, the phase diagrams can be obtained in a straightforward way from the free energy  $F$ .

For small antiferromagnetic interaction ( $K \ll t$ ), starting in the F phase and increasing the temperature  $T$ , we find a second order transition into the paramagnetic phase (P), stable at high temperature and defined by  $m = 0$  at any value of  $\theta$  (the free energy is independent of  $\theta$ ). For large antiferromagnetic coupling ( $K \gg t$ ), starting in the AF phase and increasing  $T$ , we obtain again a second order transition into the paramagnetic phase (P). In either case, a linear dependence of the critical temperature ( $T_c$ ) is obtained:  $T_c \rightarrow \pm 2K$  for  $K/t \rightarrow \infty$ .

When  $K$  and  $t$  are the same order, the competition between both takes place and different transitions can occur increasing  $T$  at low temperatures: (a) Starting from the C phase, we obtain a first order transition into AF phase. We show these transitions in Figs. 3 and 4. (b) For small values of doping  $x$ , we obtain a first-order transition from AF into F in a narrow region of the antiferromagnetic coupling. This transition is depicted in Fig. 3. (c) For  $x$  near to 0.5, at very low temperatures the phase diagram shows a second-order transition from C into P. See Fig. 4.

In conclusion, we have studied the competition between double exchange mechanisms for itinerant electrons and antiferromagnetic superexchange interaction for localized electrons. We approach the problem by truncating the Hamiltonian to reduce the Hund energy to a  $z$  component coupling and calculate Green's functions using an RPE and mean field approximation to obtain the density of states for the itinerant electrons. We have then calculated the Free energy, to obtain the different phase diagrams for different dopings. The type of magnetic order assumed makes our calculations valid only for the electron-doped manganese perovskites.

### Acknowledgements

One of us (R. A.) is supported by the Consejo Nacional de Investigaciones Científicas y Técnicas (CONICET). B.A. is partially supported by CONICET.

### References

- [1] R. von Helmholt, J. Wecker, B. Holzapfel, L. Schultz, K. Samwer, Phys. Rev. Lett. 71 (1993) 2331.
- [2] G.H. Jonker, J.H. van Santen, Physica 16 (1950) 337.
- [3] J.H. van Santen, G.H. Jonker, Physica 16 (1950) 599.
- [4] C. Zener, Phys. Rev. 82 (1951) 403.
- [5] P.W. Anderson, H. Hasegawa, Phys. Rev. 100 (1955) 675.
- [6] P.G. de Gennes, Phys. Rev. 118 (1960) 141.
- [7] K. Kubo, N. Ohata, J. Phys. Soc. Jpn 33 (1972) 21.
- [8] J. Mazzaferro, C.A. Balseiro, B. Alascio, J. Phys. Chem. Solids 46 (1985) 1339.
- [9] N. Furukawa, J. Phys. Soc. Jpn 63 (1994) 3214.
- [10] A.J. Millis, P.B. Littlewood, B.I. Shraiman, Phys. Rev. Lett. 74 (1995) 5144.
- [11] R. Allub, B. Alascio, Solid State Commun. 99 (1996) 613.
- [12] R. Allub, B. Alascio, Phys. Rev. B 55 (1997) 14113.
- [13] E.O. Wollan, W.C. Koehler, Phys. Rev. 100 (1955) 545.
- [14] J. Briático, B. Alascio, R. Allub, A. Butera, A. Caneiro, M.T. Causa, M. Tovar, Phys. Rev. B 53 (1996) 14020.
- [15] See, e.g. E.N. Economou, in: P. Fulde (Ed.), Green's Functions in Quantum Physics, Appendix B, Springer Series in Solid-State Sciences 7.
- [16] A.A. Aligia, Thesis, Instituto Balseiro, 1984.
- [17] A.A. Aligia, J. Magn. Magn. Mater. 43 (1984) 119.
- [18] D.P. Arovas, F. Guinea, preprint.
- [19] D.I. Golosov, M.R. Norman, K. Levin, cond-mat/9712094.